Modeling and Simulation of Wrinkling in Compression Molding Process of Fiber Reinforced Composites[1]

J. Fish[2], J. LeMonds[3] and K.L.Shek[2]

ABSTRACT

A model has been developed for the prediction of wrinkling during the compression molding process for composites with thick cross-sections. The onset of wrinkling is modeled as a localized bifurcation mode, which produces additional solutions in the form of wrinkles in a single layer or group of neighboring layers. Average mechanical, thermal and cure properties of the composite material needed for simulation of compression molding process are developed.

1. Research supported by General Electric Company

2. Rensselaer Polytechnic Institute

3. General Electric Company

1. Introduction

Since 1909 when Baekeland first produced thermosetting raisins, composite fabrication techniques such as compression and transfer molding of thermosetting plastics have evolved from early manual labor to fully automated system.

In a typical compression or transfer molding process, a thermosetting fiber reinforced molding compound is exposed to sufficient heat to soften or plasticize it sufficiently to flow into the mold cavity. The material is then held under pressure for a sufficient length of time to cure. In the compression molding process the pressure is introduced by moving the top half of the mold against the part.

There are a number commercial codes for the simulation of compression molding process of fiber-reinforced thermosets [1], [2]. These finite element based codes predict the mold filing, distribution of fiber orientation, shrinkage and warpage of the final part. To our knowledge none of the existing codes attempt to predict micromechanical failure mode in the form of wrinkle, which often occurs in the manufacturing of thick composite parts, nor there is any theoretical framework addressing this difficult issue. Thus the primary objective of the current paper is to develop a simulation tool aimed at predicting the onset of wrinkling during the compression molding process.

The paper is organized as follows. In Section 2, we present a wrinkling model in the form of localized instability mode. Section 3 deals with the overall thermal, mechanical and cure properties of the composite which evolve in the compression molding process. Implementation of the wrinkling model into ABAQUS via UMAT interface conclude the manuscript.

2. Wrinkling Modeling

In this section we model formation of wrinkles developed in compression molding process. Wrinkling is a localized phenomenon involving one or more layers. This mode of failure typically occurs in thick-layered composites.

Because of the localized nature of wrinkling failure we will attempt to model this mode of instability as a sequence of kinks shown in Figure 1. In this section we develop a 3D wrinkling model, which generalizes the previous work of Budiansky and Fleck [3].

2.1 Definitions and notation

We denote $(\,)^o$ and $(\,)^1$ as pre- and post- wrinkling quantities; $\boldsymbol{e}_i^o$ and $\boldsymbol{e}_i^1$ denote the unit vectors in the pre- and post- kinking coordinate system, such that $\boldsymbol{e}_1^o$ and $\boldsymbol{e}_1^1$ are pointing in the fiber direction as shown in Figure 1.

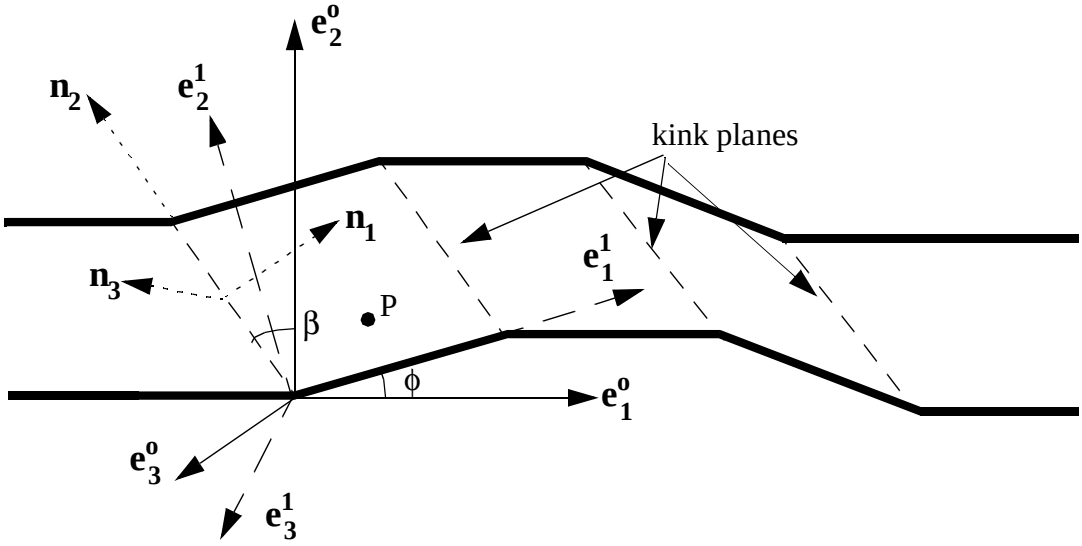

Figure 1: Wrinkling model and definition of coordinate systems

We assume that at the onset of wrinkling the rotation of $\boldsymbol{e}_i^1$ axis about $\boldsymbol{e}_i^o$ can be defined by three small angles $\phi, \theta, \psi = O(\varepsilon)$, where $0 < \varepsilon \ll 1$; ϕ is the rotation about $\boldsymbol{e}_3^o$ and $\boldsymbol{Q}(\phi)$ is a corresponding rotation matrix, such that $\boldsymbol{e}^o = \boldsymbol{Q}(\phi)\boldsymbol{e}^1$. Similarly, θ is the rotation about the new axis $\boldsymbol{e}_1^o$ and $\boldsymbol{Q}(\theta)$ is a corresponding rotation matrix, ψ is the rotation about the new axis $\boldsymbol{e}_2^o$ obtained after the first two rotations, and $\boldsymbol{Q}(\psi)$ is a corresponding rotation matrix. The relation between the pre- and post- wrinkling coordinate system is given by:

$$\boldsymbol{e}^o = \lim_{\varepsilon \to 0} \boldsymbol{Q}(\psi)\boldsymbol{Q}(\theta)\boldsymbol{Q}(\phi)\boldsymbol{e}^1 = [\boldsymbol{Q}(\psi) + \boldsymbol{Q}(\theta) + \boldsymbol{Q}(\phi)]\boldsymbol{e}^1 = \boldsymbol{Q}\boldsymbol{e}^1 \quad (1)$$

where

$$\boldsymbol{Q} = \begin{bmatrix} 1 & -\phi & -\psi \\ \phi & 1 & -\theta \\ \psi & \theta & 1 \end{bmatrix} \quad (2)$$

We further assume that the shear angle γ (shown in Figure 2) developed by rotation around the x_1^1 axis is intifisimaly small at the onset of wrinkling, i.e., $\gamma = O(\varepsilon)$. Furthermore, by exploiting the kinematics of the deformation in the wrinkling band, governed

by $\frac{d\theta}{dx_1^1} = \gamma$ and $\theta(x_1^1 = 0) = 0$, and assuming that the wrinkling band is very narrow, i.e., $x_1^1 = O(\varepsilon)$ for any point in the band, we get that $\theta = O(\varepsilon^2)$, and thus θ can be neglected compared to ψ, φ in subsequent derivations.

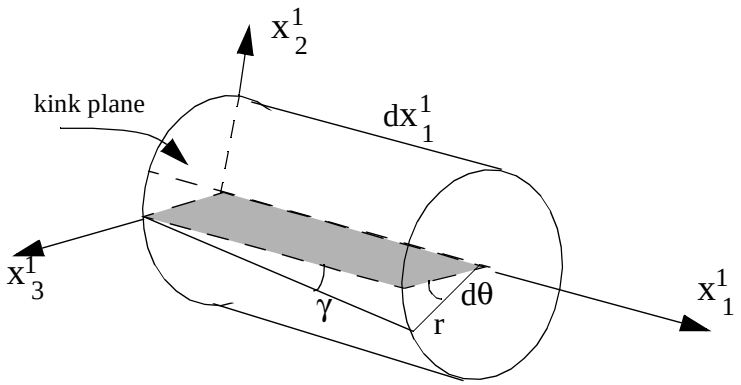

Figure 2: Kinematics of torsion around x_1^1

The unit vectors $\boldsymbol{n}_i$ defining the kink plane, such that $\boldsymbol{n}_1$ is the normal to the kink plane, can be related to the unit vectors $\boldsymbol{e}_i^o$ in terms of two rotations α, β (because $\boldsymbol{n}_2, \boldsymbol{n}_3$ are two orthogonal unit vectors arbitrary located in the plane normal to $\boldsymbol{n}_1$). Let β be the rotation angle about $\boldsymbol{e}_3^o$ and $\boldsymbol{R}(\beta)$ the corresponding rotation matrix. Likewise, let α be the rotation angle about $\boldsymbol{n}_2$ obtained after the first rotation and $\boldsymbol{R}(\alpha)$ be the corresponding rotation matrix. The overall rotation matrix $\boldsymbol{R}$, defined such that $\boldsymbol{n} = \boldsymbol{R}^T \boldsymbol{e}^o$, is given by

$$\boldsymbol{R} = \boldsymbol{R}(\alpha)\boldsymbol{R}(\beta) = \begin{bmatrix} \cos\alpha\cos\beta & -\cos\alpha\sin\beta & -\sin\alpha \\ \sin\beta & \cos\beta & 0 \\ \sin\alpha\cos\beta & -\sin\alpha\sin\beta & \cos\alpha \end{bmatrix} \tag{3}$$

2.2 Traction continuity

Continuity of tractions across the wrinkling interface can be expressed as follows:

$$\boldsymbol{e}_k^1(\sigma^1 \boldsymbol{n}_1 - \sigma^0 \boldsymbol{n}_1) = 0 \qquad k = 1, 2, 3 \tag{4}$$

Due to fiber inextension only, the traction continuity condition for $k = 2, 3$ has to be satisfied. Combining equations (2)-(4) and assuming that $abs(\alpha) \ll \pi/2$, $abs(\beta) \ll \pi/2$ yields a system of two equations:

$$\Delta\sigma_{21}\left(1 + \phi\frac{\tan\beta}{\cos\alpha} + \psi\tan\alpha\right) + \Delta\sigma_{23}(-\psi + \tan\alpha) + \Delta\sigma_{22}\left(-\phi + \frac{\tan\beta}{\cos\alpha}\right) = \phi\left(-\sigma_{11}^0 + \sigma_{22}^0 - 2\sigma_{21}^0\frac{\tan\beta}{\cos\alpha} - \sigma_{31}^0\tan\alpha\right) + \psi(\sigma_{32}^0 - \sigma_{21}^0\tan\alpha) \tag{5}$$

$$\Delta\sigma_{31}\left(1 + \psi\tan\alpha + \phi\frac{\tan\beta}{\cos\alpha}\right) + \Delta\sigma_{33}(-\psi + \tan\alpha) + \Delta\sigma_{32}\left(-\phi + \frac{\tan\beta}{\cos\alpha}\right) = \phi\left(\sigma_{32}^0 - \sigma_{31}^0\frac{\tan\beta}{\cos\alpha}\right) + \psi\left(-\sigma_{11}^0\tan\alpha + \sigma_{33}^0 - \sigma_{21}^0\frac{\tan\beta}{\cos\alpha} - 2\sigma_{31}^0\tan\alpha\right) \tag{6}$$

where $\Delta\sigma_{ij}$ is defined as:

$$\Delta\sigma_{ij} = \sigma_{ij}^1 - \sigma_{ij}^0 \tag{7}$$

We next proceed to define the kinematics of the deformation in the wrinkling band.

2.3 Kinematics of wrinkling

Consider a material point $P(\chi_1^1, \chi_2^1, \chi_3^1)$ within a wrinkling band as shown in Figure 3. The dotted lines show the fiber orientation. L denotes the distance of the point P from the kink plane measured along the fiber direction $\boldsymbol{e}_1^1$.

At the onset of wrinkling the displacement field within a wrinkling band $\boldsymbol{u}^1$ is assumed to be a small perturbation from the displacement field outside the wrinkling band $\boldsymbol{u}^0$, i.e.:

$$\boldsymbol{u}^1 = \boldsymbol{u}^0 + \Delta\boldsymbol{u} \tag{8}$$

where the perturbed displacement field $\Delta\boldsymbol{u}$ is defined as follows:

$$\Delta\boldsymbol{u} = \phi L\boldsymbol{e}_2^1 - \psi L\boldsymbol{e}_3^1 \tag{9}$$

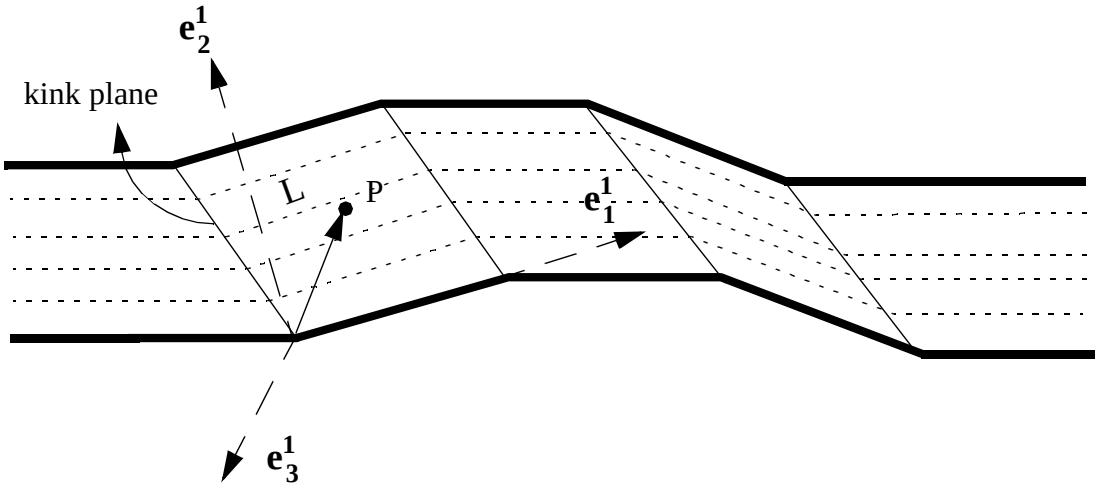

Figure 3: Wrinkling kinematics

This form of perturbation is chosen because of (i) the fiber inextension assumption, and (ii) the small rotations assumption at the onset of wrinkling. It remains to express the distance L in terms of the coordinates of the point P.

Let $ax_1^1 + bx_2^1 + cx_3^1 = 0$ be the equation of the kink plane passing through the origin, and let $x_2^1 = \chi_2^1$, $x_3^1 = \chi_3^1$ represent the equation of a fiber in the wrinkling band passing through the point P. The intersection point between the fiber and the kink plane is given by $x_1^1 = (-bx_2^1 - cx_3^1)/a$ and consequently, the value of L is given by:

$$L = \chi_1^1 + \frac{b}{a}\chi_2^1 + \frac{c}{a}\chi_3^1 \tag{10}$$

where

$$\begin{aligned} a &= \boldsymbol{n}_1 \boldsymbol{e}_1^1 \cong \cos\alpha\cos\beta \\ b &= \boldsymbol{n}_1 \boldsymbol{e}_2^1 = \sin\beta - \phi\cos\alpha\cos\beta \\ c &= \boldsymbol{n}_1 \boldsymbol{e}_3^1 = \sin\alpha\cos\beta - \psi\cos\alpha\cos\beta \end{aligned} \tag{11}$$

Substituting (11) into (10) yields

$$L = \chi_1^1 + \left(\frac{\tan\beta}{\cos\alpha} - \phi\right)\chi_2^1 + (\tan\alpha - \psi)\chi_3^1 \tag{12}$$

Let $\Delta\varepsilon_{ij}$ be the perturbed strain field defined as $\Delta\varepsilon_{ij} = \frac{1}{2}\left(\frac{\partial}{\partial\chi_j}\Delta u_i + \frac{\partial}{\partial\chi_i}\Delta u_j\right)$, then the perturbed strain components can be expressed as follows:

$$\begin{aligned}
\Delta\varepsilon_{22} &= \phi\left(\frac{\tan\beta}{\cos\alpha} - \phi\right) \\
\Delta\varepsilon_{33} &= \psi(-\tan\alpha + \psi) \\
\Delta\gamma_{21} &= 2\Delta\varepsilon_{21} = \phi \\
\Delta\gamma_{31} &= 2\Delta\varepsilon_{31} = -\psi \\
\Delta\gamma_{32} &= 2\Delta\varepsilon_{32} = \psi\left(\varphi - \frac{\tan\beta}{\cos\alpha}\right) + \phi(\tan\alpha - \psi)
\end{aligned} \tag{13}$$

2.4 Constitutive equations

We assume that wrinkling occurs in the solid phase governed by linear elasticity equations with eigenstrains:

$$\sigma_{ij}^{m} = L_{ijkl}(\varepsilon_{kl}^{m} - \mu_{kl}^{m}) \qquad m = 0, 1 \tag{14}$$

where μ_{kl}^{m} is the eigenstrain consisting of thermal and cure effects. Equation (14) implies that the components of the constitutive tensor L_{ijkl} are seen to be identical in the pre- and post- wrinkling coordinate systems. Furthermore, we assume that because of weak coupling between mechanical thermal and cure fields, the eigenstrains on both sides of the kink plane are identical, i.e., $\mu_{kl}^{0} = \mu_{kl}^{1}$. Based on these assumptions equation (14) can be recast into the following form:

$$\Delta\sigma_{ij} = L_{ijkl}\Delta\varepsilon_{kl} \tag{15}$$

For transverse isotropic material equation (15) reduces to:

$$\begin{aligned}
&\Delta\sigma_{22} = D_a\Delta\varepsilon_{22} + D_t\Delta\varepsilon_{33} \qquad \Delta\sigma_{33} = D_t\Delta\varepsilon_{22} + D_a\Delta\varepsilon_{33} \\
&\Delta\sigma_{23} = G_t\Delta\gamma_{23} \qquad \Delta\sigma_{13} = G_a\Delta\gamma_{13} \qquad \Delta\sigma_{12} = G_a\Delta\gamma_{12}
\end{aligned} \tag{16}$$

2.5 Wrinkling condition in 3D

Substituting equations (13), (15) and (16) into (5) and (6) and neglecting $O(\varepsilon^2)$ terms yields a homogeneous system of equations for ϕ and ψ:

$$\begin{bmatrix} A & B \\ C & D \end{bmatrix} \begin{bmatrix} \phi \\ \psi \end{bmatrix} = \begin{bmatrix} 0 \\ 0 \end{bmatrix} \tag{17}$$

where

$$\begin{aligned} A &= G_a + G_t(\tan\alpha)^2 + D_a\frac{(\tan\beta)^2}{(\cos\alpha)^2} + \sigma_{11}^0 - \sigma_{22}^0 + 2\sigma_{21}^0\frac{\tan\beta}{\cos\alpha} + \sigma_{31}^0\tan\alpha \\ B &= -(G_t + D_t)\frac{\tan\alpha\tan\beta}{\cos\alpha} - \sigma_{32}^0 + \sigma_{21}^0\tan\alpha \\ C &= (D_t + G_t\cos\alpha)\frac{\tan\alpha\tan\beta}{\cos\alpha} - \sigma_{32}^0 + \sigma_{31}^0\frac{\tan\beta}{\cos\alpha} \\ D &= -G_a - D_a(\tan\alpha)^2 - G_t\frac{(\tan\beta)^2}{\cos\alpha} + \sigma_{11}^0 - \sigma_{33}^0 + \sigma_{21}^0\frac{\tan\beta}{\cos\alpha} + 2\sigma_{31}^0\tan\alpha \end{aligned} \tag{18}$$

Thus the condition for wrinkling may be stated as follows:

$$F(\alpha, \beta) = A \cdot D - B \cdot C = 0 \tag{19}$$

2.6 Wrinkling condition in 2D

Reduction to 2D case can be obtained by forcing the normal to the kink plane and the fiber orientation in the wrinkling band to be aligned in the $x_1 - x_2$ plane, i.e., $\alpha = \psi = 0$. Furthermore, transverse shear stress components are assumed to be negligible, i.e., $\sigma_{13} = \sigma_{23} = 0$. In this case the wrinkling condition degenerates to:

$$A(\beta) = G_a + D_a(\tan\beta)^2 + \sigma_{11}^0 - \sigma_{22}^0 + 2\sigma_{21}^0\tan\beta = 0 \tag{20}$$

It can be seen that in absence of stresses $A > 0$. As the thermomechanical loading increases, and the values of stresses approach those of the material constants, the value of $A(\beta)$ may decrease and finally approach zero, which is an indication of the onset of wrinkling. In this process the critical value of β is the minimizer of $A(\beta)$:

$$\frac{\partial A}{\partial \beta} = 0 \Rightarrow \tan\beta = -\frac{\sigma_{21}^0}{D_a}$$
$$\frac{\partial^2 A}{\partial \beta^2}\left(\tan\beta = -\frac{\sigma_{21}^0}{D_a}\right) = \frac{D_a}{(\cos\beta)^4} > 0 \Rightarrow min \tag{21}$$

The minimal value of $A(\beta)$ is given by:

$$A_{min} = G_a - F(\sigma^0) \tag{22}$$

where

$$F(\sigma^0) = \sigma_{22}^0 - \sigma_{11}^0 + \frac{(\sigma_{21}^0)^2}{D_a} \tag{23}$$

To measure the proximity to wrinkling failure it is convenient to define the wrinkling parameter $\Im$ as follows:

$$\Im = F/G_a = \frac{\sigma_{22}^0 - \sigma_{11}^0}{G_a} + \frac{(\sigma_{21}^0)^2}{D_a G_a} \tag{24}$$

where F and G_a represent the forcing function and resistance to wrinkling, respectively. Note that at the onset of wrinkling $\Im = 1$.

3. Simulation of the compression moulding process

In order to simulate the compression molding process it is necessary to find the overall properties of the preform material as a function of temperature and cure. For this purpose we will first estimate the overall mechanical, thermal and cure properties of a single layer, which we will subsequently refer to as micromechanical homogenization. In practice however, compression molding of thick composites often involves hundreds of layers, and thus in the second stage we will compute the average material properties of sublaminate, which we will refer to as mesomechanical homogenization.

3.1 Micromechanical homogenization with eigenstrains

To estimate the overall mechanical, thermal and cure properties of a single layer we will employ the mathematical homogenization theory with eigenstrains recently developed in [4]. We will briefly summarize the theory and extend its use to cure and thermal strains, which will be collectively referred to as eigenstrains in an otherwise elastic body. Attention will be restricted to small deformations.

We assume that the microstructure of the composite is periodic so that the homogenization process can be performed in a unit cell domain, denoted by ω. Thus, the response functions, such as displacements and stresses, are also periodic. Let x be a coordinate vector on the mesoscale, and $y \equiv x/\varsigma$ be a microscopic position vector where ς is a small parameter representing the ratio between the scales. For any periodic function $f^{\varsigma}(x) = f(x, y(x))$, the indirect microscopic spatial derivatives of f^{ς} can be calculated by the chain rule as

$$f^{\varsigma}_{,x_i}(x) = f_{,x_i}(x, y) + \frac{1}{\varsigma} f_{,y_i}(x, y) \tag{25}$$

where subscripts followed by a comma denote partial derivatives with respect to the subscript variables (i.e., $f^{\varsigma}_{,x_i} = \dfrac{\partial f^{\varsigma}}{\partial x_i}$).

In modeling a heterogeneous medium, micro-constituents are assumed to possess homogeneous properties and satisfy the set of continuum mechanics equations

$$\sigma^{\varsigma}_{ij,\,x_j} + b_i = 0 \qquad \sigma^{\varsigma}_{ij} = L_{ijkl}(\varepsilon^{\varsigma}_{kl} - \mu^{\varsigma}_{kl}) \qquad \varepsilon^{\varsigma}_{ij} = \left(u^{\varsigma}_{i,\,x_j} - u^{\varsigma}_{j,\,x_i}\right)/2 \tag{26}$$

and the appropriate boundary and interface conditions. In (26), the eigenstrain tensor consists of thermal μ^{th} and cure shrinkage μ^{cs} strains can be expressed by:

$$\mu_{ij}(x, y, T, \theta) = \mu^{th}_{ij}(x, y, T) + \mu^{cs}_{ij}(x, y, T, \theta) \tag{27}$$

where T and θ are temperature and cure fields, respectively. In the present work we assume that evolution of thermal strains $\mu^{th}_{ij}(T)$, cure shrinkage strains $\mu^{cs}_{ij}(T, \theta)$, and constitutive tensor $L_{ijkl}(T, \theta)$ in a pure raisin material can be measured experimentally. Furthermore, we assume that cure and thermal effects are negligible in the fiber.

Both displacements and strains are approximated using a double scale asymptotic expansion of the form:

$$u_i = u^0_i(x, y) + \varsigma u^1_i(x, y) + \ldots, \qquad \mu_{ij} = \mu^0_{ij}(x, y) + \varsigma \mu^1_{ij}(x, y) + \ldots \tag{28}$$

The corresponding expansion for the strain and stress tensors can be obtained by combining the above expansions with the governing equations and by exploiting the indirect differentiation rule:

$$\varepsilon_{ij}(x,y) \approx \frac{1}{\varsigma}\varepsilon_{ij}(x,y) + \varepsilon_{ij}(x,y) + \varsigma\varepsilon_{ij}(x,y) + \ldots$$
$$\sigma_{ij}(x,y) \approx \frac{1}{\varsigma}\sigma_{ij}(x,y) + \sigma_{ij}(x,y) + \varsigma\sigma_{ij}(x,y) + \ldots \tag{29}$$

Various order of stress and strain tensors are related by the constitutive equation:

$$\sigma_{ij}^{-1} = L_{ijkl}\varepsilon_{kl}^{-1}, \qquad \sigma_{ij}^{r} = L_{ijkl}(\varepsilon_{kl}^{r} - \mu_{kl}^{r}) \qquad r = 0, 1\ldots \tag{30}$$

Substituting equation (30) into the equilibrium equation, a set of equilibrium equations for various orders of ς can be obtained. From the lower order $O(\varsigma^{-2})$ equilibrium, we get a classical estimate: $u_i^0 = u_i^0(x)$. Following reference [4] $O(\varsigma^{-1})$ the equilibrium equation provides two governing equations for the unit cell problem in ω:

$$\{L_{ijkl}(\delta_{km}\delta_{lr} + \Psi_{klmr})\}_{,y_j} = 0$$
$$(L_{ijkl}\Psi_{klmn})_{,y_j} d_{mn}^{\mu} - (L_{ijkl}\mu_{kl}^{0})_{,y_j} = 0 \tag{31}$$

where δ_{km} is the Kronecker delta, Ψ_{klmn} is related to the elastic strain concentration factor A_{klmn} as shown in equation (32). The microscopic strain can be written in terms of the overall mesoscopic strain tensor $\bar{\varepsilon}_{mn}$ as follows:

$$\varepsilon_{kl} = A_{klmr}\bar{\varepsilon}_{mr} \qquad A_{klmr} = \frac{1}{2}(\delta_{km}\delta_{lr} + \delta_{kr}\delta_{lm}) + \Psi_{klmr} \tag{32}$$

In the following, we will adopt a matrix notation such that $\boldsymbol{A}$ is the matrix representation of A_{klmn}. The first part in equation (31) represents a classical linear unit cell or inclusion problem. Either finite element method or analytical solution of the inclusion problem can be used for calculation of stress/strain concentration factors. In the present work Mori-Tanaka method [5], [6] is adopted for calculation of strain concentration factors.

The elastic homogenized stiffness tensor $\bar{\boldsymbol{L}}$ follows directly from the $O(\varsigma^{0})$ equilibrium equation and is given as follows:

$$\bar{\boldsymbol{L}} = \frac{1}{|\omega|}\int_{\omega} \boldsymbol{L}\boldsymbol{A}\, d\omega = \frac{1}{|\omega|}\int_{\omega} \boldsymbol{A}^{T}\boldsymbol{L}\boldsymbol{A}\, d\omega \tag{33}$$

where $|\omega|$ is the unit cell volume.

Separation of variables for the eigenstrain field $\mu_{\eta}^{0}(x,y) = \sum_{\eta} \psi_{\eta}(y)\mu_{\eta}^{0}(x)$ combined with the expression for d^{μ} obtained from the second equation in (31) yields a closed form expression for the microstrain field in a unit cell domain expressed in terms of the overall strain field and the eigenstrain field $\mu^{0}(x)$:

$$\varepsilon(x,y) = \boldsymbol{A}(y)\bar{\varepsilon}(x) + \sum_{\eta} \boldsymbol{D}_{\eta}(y)\mu_{\eta}^{0}(x) \tag{34}$$

where $\boldsymbol{D}_{\eta}(y)$ is the eigenstrain influence function given in terms of strain concentration function $\Psi(y)$ as follows:

$$\boldsymbol{D}_{\eta}(y) = \frac{1}{|\omega|}\Psi(\tilde{\boldsymbol{L}} - \bar{\boldsymbol{L}})^{-1}\int_{\omega} \Psi^{T}\boldsymbol{L}\psi_{\eta}\, d\omega \tag{35}$$

We now consider a two phase media, consisting of matrix and reinforcement, with respective volume fractions c_m and c_f. For simplicity, we assume that eigenstrains in the resin are uniformly distributed, and negligible in the fiber phase. Consequently, equations (34), (35) and (33) reduce to:

$$\varepsilon_r = \boldsymbol{A}_r\bar{\varepsilon} + \boldsymbol{D}_{rm}\mu_m \ldots\ldots\ldots r = m, f \tag{36}$$

$$\boldsymbol{D}_{rm} = (\boldsymbol{I} - \boldsymbol{A}_r)(\boldsymbol{L}_m - \boldsymbol{L}_f)^{-1}\boldsymbol{L}_m \ldots\ldots\ldots r = m, f \tag{37}$$

$$\bar{\boldsymbol{L}} = c_m\boldsymbol{L}_m\boldsymbol{A}_m + c_f\boldsymbol{L}_f\boldsymbol{A}_f \tag{38}$$

Finally, the overall stress $\bar{\sigma}$ field in the two phase material is given by

$$\bar{\sigma} = c_m\sigma_m + c_f\sigma_f = \bar{\boldsymbol{L}}\bar{\varepsilon} + \boldsymbol{V}_m\mu_m \tag{39}$$

where

$$\boldsymbol{V}_m = c_m\boldsymbol{L}_m(\boldsymbol{D}_{mm} - \boldsymbol{I}) + c_f\boldsymbol{L}_f\boldsymbol{D}_{fm} \tag{40}$$

It is important to note that concentration factors $\boldsymbol{A}_r$ computed using Mori-Tanaka scheme are functions of temperature and cure since resin properties depend on temperature and cure. Equations (36)-(39) provide the overall stresses and strains in a layer and serve as basis for linearization aimed at computing the tangent stiffness matrix.

Linearization of (39) yields:

$$\dot{\bar{\sigma}} = \bar{L}(T, \theta)\dot{\bar{\varepsilon}} + \bar{G}(T, \theta)\dot{T} + \bar{K}(T, \theta)\dot{\theta} \tag{41}$$

where

$$\bar{L} = \bar{\boldsymbol{L}} \qquad \bar{G} = \left(\frac{\partial}{\partial T}\bar{\boldsymbol{L}}\right)\bar{\varepsilon} + \frac{\partial}{\partial T}(\boldsymbol{V}_m\mu_m) \qquad \bar{K} = \left(\frac{\partial}{\partial \theta}\bar{\boldsymbol{L}}\right)\bar{\varepsilon} + \frac{\partial}{\partial \theta}(\boldsymbol{V}_m\mu_m) \tag{42}$$

3.2 Mesomechanical homogenization

Let $\dot{\sigma}^i, \dot{\varepsilon}^i, \dot{T}^i, \dot{\theta}^i, L^i, G^i, K^i$ be the rate of stress, strain, temperature and cure fields, as well as instantaneous mechanical, thermal and cure properties of a single layer i expressed in a fixed sublaminate coordinate system. These quantities are obtained by transforming the overall micromechanical fields computed in the previous section from the fiber coordinate system into a fixed coordinate system attached to a sublaminate.

Since each layer is assumed to be very thin, it is convenient to adopt a VFD (vanishing fiber diameter) averaging model, developed by Dvorak and Bahei-El-Din [7] in the context of micromechanical homogenization. In the following we generalize this model to account for thermal and cure strains and apply it to evaluate the overall properties of the sublaminate.

In this section our goal is to evaluate the instantaneous sublaminate (macroscopic) mechanical, thermal and cure material properties, denoted as L, G, K, which represent the rate form of the sublaminate constitutive equation:

$$\dot{S} = L\dot{E} + G\dot{T} + K\dot{\Theta} \tag{43}$$

where $\dot{S}, \dot{E}, \dot{T}, \dot{\Theta}$ are the sublaminate rate of stress, strain, temperature and cure fields. Mesomechanical homogenization procedure is based on the following four assumptions:

(i) Traction continuity between the layers in the sublaminate

$$\dot{\sigma}^k_{i3} = \dot{S}_{i3} \ldots\ldots i = 1, 2, 3 \tag{44}$$

where subscript 3 denotes the direction normal to the interface between the layers within a sublaminate.

(ii) Strain compatibility between the layers in the sublaminate

$$\dot{\varepsilon}^{k}_{\alpha\beta} = \dot{E}_{\alpha\beta} \ldots\ldots \alpha, \beta = 1, 2 \tag{45}$$

(iii) Temperature and cure continuity between the layers in the sublaminate

$$\dot{T}^{k} = \dot{T} \qquad \dot{\theta}^{k} = \dot{\Theta} \tag{46}$$

(iv) Application of the averaging rule for the remaining stress and strain components not included in equations (44) and (45):

$$\dot{S}_{\alpha\beta} = \sum_{k} c^{k} \dot{\sigma}^{k}_{\alpha\beta} \ldots\ldots \alpha, \beta = 1, 2 \qquad \dot{E}_{i3} = \sum_{k} c^{k} \dot{E}^{k}_{i3} \ldots\ldots i = 1, 2, 3 \tag{47}$$

where c^{k} is volume fraction of a layer calculated as a ratio of layer's thickness to sublaminate thickness. Note that the averaging rule (47) directly follows from $O(1)$ equilibrium equation [4].

For subsequent derivations we will define the following vectors:

$$\dot{e}^{k} = \begin{bmatrix} \dot{\sigma}^{k}_{\alpha\beta} \\ \dot{E}^{k}_{i3} \end{bmatrix} \qquad \dot{g}^{k} = \begin{bmatrix} \dot{\sigma}^{k}_{i3} \\ \dot{\varepsilon}^{k}_{\alpha\beta} \end{bmatrix} \equiv \begin{bmatrix} \dot{S}_{i3} \\ \dot{E}_{\alpha\beta} \end{bmatrix} = \dot{g} \tag{48}$$

To evaluate the instantaneous material properties L, G, K we devise a three step computational procedure:

Step 1: Given the constitutive equation of a layer k,

$$\dot{\sigma}^{k} = L^{k} \dot{\varepsilon}^{k} + G^{k} \dot{T}^{k} + K^{k} \dot{\theta}^{k} \tag{49}$$

find the relation between $\dot{e}^{k}$, $\dot{g}$, $\dot{T}$, and $\dot{\theta}$, i.e., determine R^{k}, H^{k}, P^{k} such that

$$\dot{e}^{k} = R^{k} \dot{g}^{k} + H^{k} \dot{T}^{k} + P^{k} \dot{\theta}^{k} \tag{50}$$

Due to the arbitrariness of thermal, mechanical and cure fields, we first set $\dot{T}^k = \dot{T} = 0$, $\dot{\theta}^k = \dot{\Theta} = 0$ and $\dot{g}^k = \dot{g}$. Then, substituting the above expressions into the constitutive equation (49) yields a set of six equations for $\dot{g}$ and $\dot{e}^k$. Assuming that L^k is nonsingular, it is feasible to express $\dot{e}^k$ in terms of $\dot{g}$, which in turn yields the expression for R^k. Similarly, we substitute $\dot{T}^k = \dot{T}$, $\dot{\theta}^k = \dot{\Theta} = 0$ and $\dot{g}^k = \dot{g} = 0$ into equation (49), which yields six equations for $\dot{e}^k$ and $\dot{T}$, and ultimately the expression H^k. Finally, P^k is found by inserting $\dot{T}^k = \dot{T} = 0$, $\dot{\theta}^k = \dot{\Theta}$ and $\dot{g}^k = \dot{g} = 0$ into (49).

Step 2: Given the layer-wise properties R^k, H^k, P^k, find the overall sublaminate properties R, H, P, such that

$$\dot{e} = R\dot{g} + H\dot{T} + P\dot{\Theta} \tag{51}$$

The sublaminate properties R, H, P can be obtained by inserting equations (47) and (48) into equation (51) which yields:

$$(R, H, P) = \sum_k c^k (R^k, H^k, P^k) \tag{52}$$

Step 3: Given the sublaminate properties R, H, P, find L, G, K relating the quantities $\dot{S}, \dot{E}, \dot{T}, \dot{\Theta}$ as shown in equation (43).

We first substitute $\dot{T} = 0$, $\dot{\Theta} = 0$ into (51), which yields six equations for $\dot{S}, \dot{E}$ and consequently the expression for L. Similarly, inserting $\dot{\Theta} = 0$ and $\dot{E} = 0$ into (51), yields G, and likewise inserting $\dot{T} = 0$ and $\dot{E} = 0$ into (51) yields K.

Remark: The plane strain case can be obtained by substituting $\dot{E}_{i3} = 0$ into (43).

4. Implementation

Both the homogenization and wrinkling prediction procedures have been implemented within the UMAT interface of ABAQUS. Figure 4 schematically shows the computational

cycle consisting of five modules implemented within UMAT in addition to ABAQUS as analysis engine.

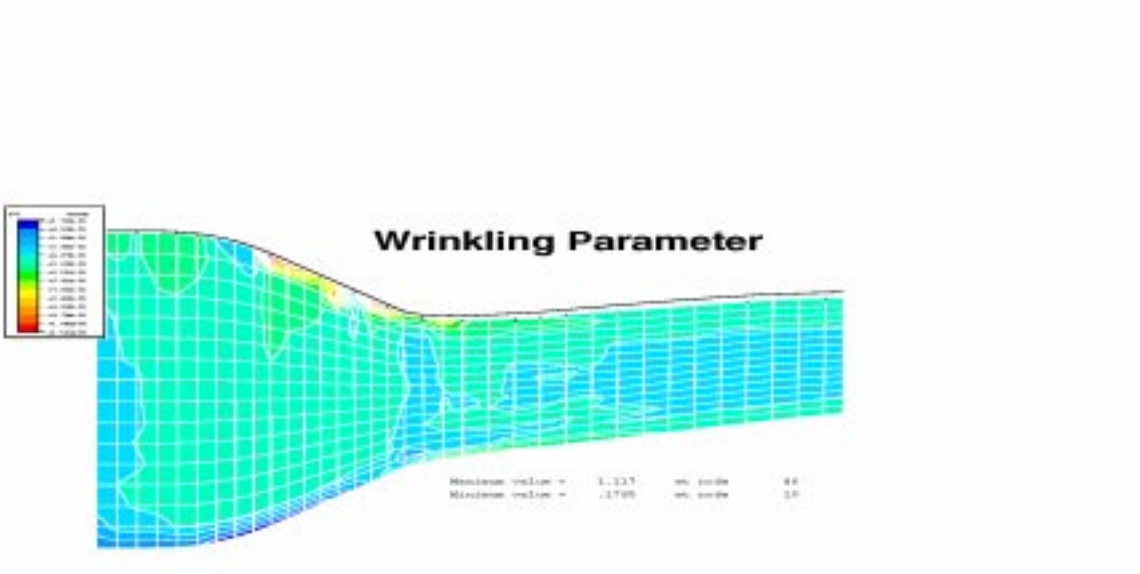

Figure 4: Compression molding process simulation with ABAQUS

The computational process starts by carrying out micromechanical homogenization of mechanical, thermal and cure properties based on mathematical homogenization procedure with eigenstrains described in Section 3.1. This module provides an overall properties for each ply. Since there would likely be numerous plies in a real part it is not feasible to represent the kinematics of each ply for a coupled thermomechanical analysis. Hence the second module performs ply-by-ply homogenization (Section 3.2). Subsequently, a typical representative cross-section is selected and an equivalent 2D properties are evaluated. Once the instantaneous material properties have been evaluated, a single iteration of the coupled thermo-mechanical analysis takes place. Results on the mesomechanical level (stresses and instantaneous material properties) are then post-processed for each Gauss point in a ply. A single computational cycle is completed by carrying out the wrinkling analysis for each Gauss point within each ply (Section 2). The value of the current wrinkling parameter is stored in the ABAQUS database.

5. Conclusions

A comprehensive model has been developed for the prediction of wrinkling in composite parts which have complex geometries and complex material behavior. The method has been implemented in ABAQUS and applied to an experiment at the General Electric company which is proprietary and cannot be presented here. The wrinkle prediction technique presented here yielded the time of the onset of wrinkling which agreed well with the experimental results and gave the location of the wrinkles in exact agreement with the experiment.

References

1 CADPRESS, The Madison Group: Polymer Processing Research Corporation.

2 MOLDFLOW, Moldflow Pty. Ltd., 259 Colchester Rd., Kilsyth, Melbourne VIC 3137, Australia.

3 B.Budiansky and N.A.Fleck, "Compressive Failure of Fibre Composites," *J. Mech. Phys. Solids*, Vol. 41, No. 1, pp. 183-211, 1993.

4 J. Fish, K.L.Shek, M. Pandheeradi, M.S. Shephard, "Computational Plasticity for Composite Structures Based on Mathematical Homogenization: Theory and Practice," *Computer Methods in Applied Mechanics and Engineering*," Vol. 148, pp. 53-73, 1997.

5 T. Mori and K.Tanaka, "Average stress in matrix and average elastic energy of materials with misfitting inclusion," *Acta Metal.*, Vol. 21, pp. 571-574, 1973.

6 Y. Benveniste, "A new approach to the application of Mori-Tanaka's theory in composite materials," *Mech. of Materials*, Vol. 6, pp. 147-157, 1987.

7 G.J. Dvorak and Y.A. Bahei-El-Din, "Plasticity Analysis of Fibrous Composites," *Journal of Applied Mechanics*, Vol. 49, pp. 327-335, 1982.